# CHAPTER V
# HYDROXYAPATITE/OVALBUMIN COMPOSITE PARTICLES AS MODEL PROTEIN CARRIERS FOR BONE TISSUE ENGINEERING: II. RELEASE OF OVALBUMIN

## 5.1 Abstract

Different starting materials (natural and chemical substances) were employed for synthesizing hydroxyapatite (HAp) particles as a protein carrier. Egg ovalbumin (OVA), the main constituent of egg white with high functionality including modifying HAp properties, was used as a model protein. HAp particles were prepared via a co-precipitation method with various amounts of OVA (i.e., 1, 2, and 3g/500 mL solution) and pH conditions (i.e., 7 and 9); also, the chemical properties of the obtained HAp particles were investigated. The incorporated and released amounts of OVA from the HAp/OVA particles were examined. Both incorporated and released OVA contents slightly increase with increasing the initial amount of OVA, but significantly increase with lowering pH value. Besides, a larger number of OVA incorporated and released were observed in the obtained carriers synthesized from the chemical starting material compared to the natural one. The released profiles demonstrated a slowly releasing behavior within 21 days, followed by a plateau release without the initial bursting, suggesting that the OVA release was clearly prolonged by the incorporation. This release characteristic could be promising for bone tissue engineering applications.

(**Key-words**: Hydroxyapatite; Ovalbumin; Composite particles)

## 5.2 Introduction

To be bone substitutes as orthopedic or dental prostheses, artificial materials with the chemical and morphological similarity to the natural bone are required (Sopyan, 2007; Carutenuto, 1999). A large number of biomaterials have been widely investigated as the synthetic bone substitutes (Kokubo *et al.*, 2003). Owing to its

mineral phase resemblance to human bone, Hydroxyapatite (HAp), one of calcium phosphate (CaP) based ceramic materials, has been applied in various medical applications such as dental implants, drug delivery systems, and so forth. More importantly, this bioactive ceramic is the best for inducing osteogenesis and new bone formation in soft tissues (Wang, 2007; Krisanapiboon, 2006).

Considering the several utilizations of HAp in clinical fields, many preparation methods of HAp particles, including electrochemical synthesis (Djosic *et al.*, 2008), reflux procedure (Ye *et al.*, 2008), capillary microfluidic technique (Shum *et al.*, 2009), hydrothermal treatment (Wang *et al.*, 2006), microemulsion route (Koumoulidis *et al.*, 2003), precipitation (Santos and Viswanath, 2008), and sol-gel approach (Bose *et al.*, 2003) have been reported. Besides, numerous biosurfactants have also been presented to be efficient templates for particle size, shape, and morphology. For instance, yeast cells, sucrose, and even proteins were employed as template materials to improve the surface area and the formation of the HAp particles (Bose, 2003; He, 2010; Zhao, 2008). Among them, the proteins have been documented to have better biocompatibility and more sufficient hemostatic properties (Sivakumar *et al.*, 2002). Thus, the combination of proteins on apatite forms has been extensively studied to analyze the protein-released characteristics for enhancing osteoinduction (Liu *et al.*, 2001). Egg ovalbumin (OVA), a stable and inexpensive protein readily extracted from egg white, can lead to either controlled HAp growths or modified HAp properties. With its functional groups, this phosphoglycoprotein has strong negative dipoles to chelate the free $Ca^{2+}$ cations in calcium phosphate solution (Zhao *et al.*, 2008). Hence, it is of interest to incorporate OVA during HAp formation to generate protein carriers for the release applications.

Herein, we performed two kinds of starting materials with various OVA contents (i.e., 1, 2, and 3 g/500 mL solution) and pH values (i.e., 7 and 9) through a simple co-precipitation method for OVA-incorporated HAp (HAp/OVA) synthesis. Firstly, we purpose egg shells (CaO) as a calcium source and $H_3PO_4$ as a phosphorous source. Secondly, Calcium carbonate ($CaCO_3$) and Calcium hydrogen phosphate dihydrate ($CaHPO_4.2H_2O$) were used as calcium and phosphorous sources, respectively. The comparative studies of these two cases OVA carriers were evaluated. Also, the loaded capacities and release kinetics of OVA were examined.

## 5.3 Experimental

### 5.3.1 Materials

All chemical reagents including calcium hydrogen phosphate dihydrate ($CaHPO_4.2H_2O$, A.R. grade, Fluka), calcium carbonate ($CaCO_3$, A.R. grade, Carlo Erba), nitric acid ($HNO_3$, A.R. grade, Labscan), phosphoric acid ($H_3PO_4$, A.R. grade, Labscan), tris (hydroxymethyl)-aminomethane (tris-base, A.R. grade, Sigma), and egg ovalbumin (OVA, grade II, Sigma-Aldrich) were used without further purification. CaO from egg shells was prepared following the previous report of Rivera *et al.* (1999).

### 5.3.2 Synthesis of Hydroxyapatite/Ovalbumin Composite Particles

HAp and HAp/OVA particles were prepared by co-precipitation method. In the typical procedure, 2.00 g of $CaHPO_4.2H_2O$ (as a phosphorous source) and 0.79 g of $CaCO_3$ (as a calcium source) were dissolved in 1 M $HNO_3$ 25 ml under gentle stirring at 70 °C for 2 h and the pH of the solution was kept to 2. OVA were subsequently added in the initial amounts of 1, 2, and 3 g/500 mL of the mixed solution at room temperature. 200 mL of 1 M and 2 M tris-base solution were then poured into the mixture generating the precipitation at pH 7 and pH 9, respectively. The precursor solution was stirred vigorously to yield a homogeneous product. The product was then filtered off and washed several times with deionized water. After centrifugation, the resulting material was freeze-dried for 48 h to obtain the fine powder products. The similar process with the use of 1.25 g of CaO and 1.50 g of $H_3PO_4$ as calcium and phosphorous sources, respectively, was performed for comparison. With many conditions mentioned above, the sample names were specified as shown in Table 5.1.

**Table 5.1** Experimental conditions of HAp and HAp/OVA particles

| Starting Material | Initial Amount of OVA (g) | pH Condition | Sample Name |
|---|---|---|---|
| $CaCO_3$ + | 0 | 7 | 0D-7 |
| $CaHPO_4.2H_2O$ | 1 | 7 | 1D-7 |
| | 2 | 7 | 2D-7 |
| | 3 | 7 | 3D-7 |
| | 0 | 9 | 0D-9 |
| | 1 | 9 | 1D-9 |
| | 2 | 9 | 2D-9 |
| | 3 | 9 | 3D-9 |
| CaO (Egg Shells) + | 0 | 7 | 0E-7 |
| $H_3PO_4$ | 1 | 7 | 1E-7 |
| | 2 | 7 | 2E-7 |
| | 3 | 7 | 3E-7 |
| | 0 | 9 | 0E-9 |
| | 1 | 9 | 1E-9 |
| | 2 | 9 | 2E-9 |
| | 3 | 9 | 3E-9 |

5.3.3 Characterization

The crystallographic phases of the HAp/OVA particles were analyzed by X-ray diffractometer (WDXRD, D/MAX 2000 series Rigaku) with an incident X-ray wavelength of 1.54 Å (Cu Kα line) at the scanning rate of 0.02° per minute over a range of 2θ from 5° to 60° with JCPDS database (9-432). Fourier transform infrared (FT-IR) spectrograph carried out on a Nicolet Nexus spectrometer (NEXUS 670, Nicolet) was performed using the KBr pellet technique, working in the wavelength from 4000 to 400 $cm^{-1}$. The structural morphology images were recorded on a transmission electron microscope (TEM, JEM-2100, JEOL) with an acceleration

voltage of 200 kV. Energy dispersive X-ray (EDX) element analysis of the samples was also investigated with scanning electron microscope (SEM, JSM-5410LV, JEOL) operated at 15 kV. The average pore diameters of the obtained particles were taken on autosorb-1 instrument (AS-1, Quantachrome) using physisorption of nitrogen at temperature of 77 K. Thermogravimetric analysis (TGA, TGA7, Perkin Elmer) was carried out on the dried samples (5 mg) to examine the relative amount of OVA incorporated in HAp particles with a heating rate 10°/min under a flowing air atmosphere.

#### 5.3.4 Release Kinetics of Ovalbumin

About 20 mg of HAp and HAp/OVA particles were immersed in 10 ml phosphate buffer solution at pH 7.4, in which matches the normal body and blood system of a human being. The controlled release systems were shaken in the water bath with a stirring rate of 70 rpm at 37 °C. The amount of OVA released in the supernatant was measured at various time points by UV-VIS spectrophotometer (UV-1800) at the wavelength of 280 nm through the use of a pre-determined standard calibration curve. Furthermore, the gravimetric analysis was used to confirm the amount of OVA lost after 21 days.

#### 5.3.5 Statistical Analysis

All quantitative examinations were collected in triplicate and the results were presented as means and standard deviations. Significance between the mean values was determined by ANOVA one-way analysis using Tukey's test for variances at a 95% confidence level.

## 5.4 Results and Discussion

#### 5.4.1 Material Characterization

The formation of HAp particles was ascertained by X-ray diffraction (XRD) analysis. The XRD patterns of the HAp/OVA particles with particular peaks ascribed to the lattice constant of HAp according to the JCPDS (9-432) were in given in the comparative chart of Figure 5.1. From the results, the presence of the OVA

during the synthesis does not have an influence on the structural development of HAp. Besides, no difference in HAp/OVA characteristic diffraction peaks was perceived for all cases given above. These XRD data also show poorly-crystallized traces of the powders due to water sublimation in the freeze-drying process (Jalota *et al.*, 2007), resulting in estimated crystallite sizes. Calculations of the crystallite size using the Scherrer equation were performed for the (002) reflection peak corresponding to $2\theta = 26^{\circ}$ because of well resolved characteristics (Suru *et al.*, 2005). The mean sizes of crystallites are within the range of 16–20nm.

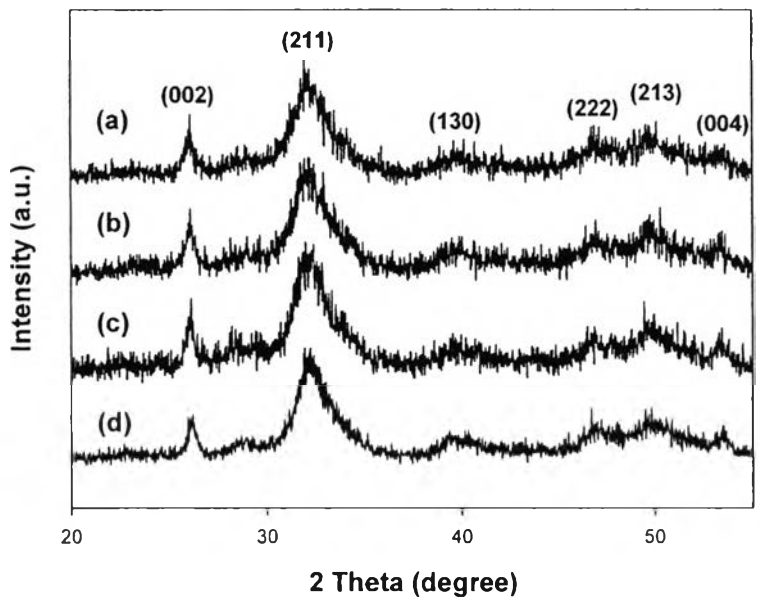


**Figure 5.1** XRD patterns of (a) 1D-7, (b) 1D-9, (c) 1E-7, and (d) 1E-9.

Figure 5.2 exhibits the FT-IR spectra of the HAp/OVA particles. The IR spectra of pure OVA and HAp are also shown for comparison. The OVA spectrum displayed the typical bands at 3299 $cm^{-1}$, 1652 $cm^{-1}$, 1539 $cm^{-1}$, and 1457 $cm^{-1}$ represented to the nitrogen-hydrogen stretch (N-H), the carbonyl vibration (C=O), the carbon-nitrogen vibration (C-N), and the stretching vibration of carbon-hydrogen (C-H), respectively (Zhao *et al.*, 2008). The spectrum of pure HAp demonstrates the adsorption bands at 3569 $cm^{-1}$ assigned to OH stretching, 1630 $cm^{-1}$

assigned to OH vibration of the apatitic group, 1035 $cm^{-1}$ assigned to $PO_4^{3-}$ stretching vibration, as well as 601 $cm^{-1}$ and 563 $cm^{-1}$ assigned to $PO_4^{3-}$ deformation vibration (Suwa, 1993; Xu, 2007). The bands at 1654 $cm^{-1}$ and 1539 $cm^{-1}$ of HAp/OVA spectra, therefore, ascertained that OVA were incorporated in the HAp particles.

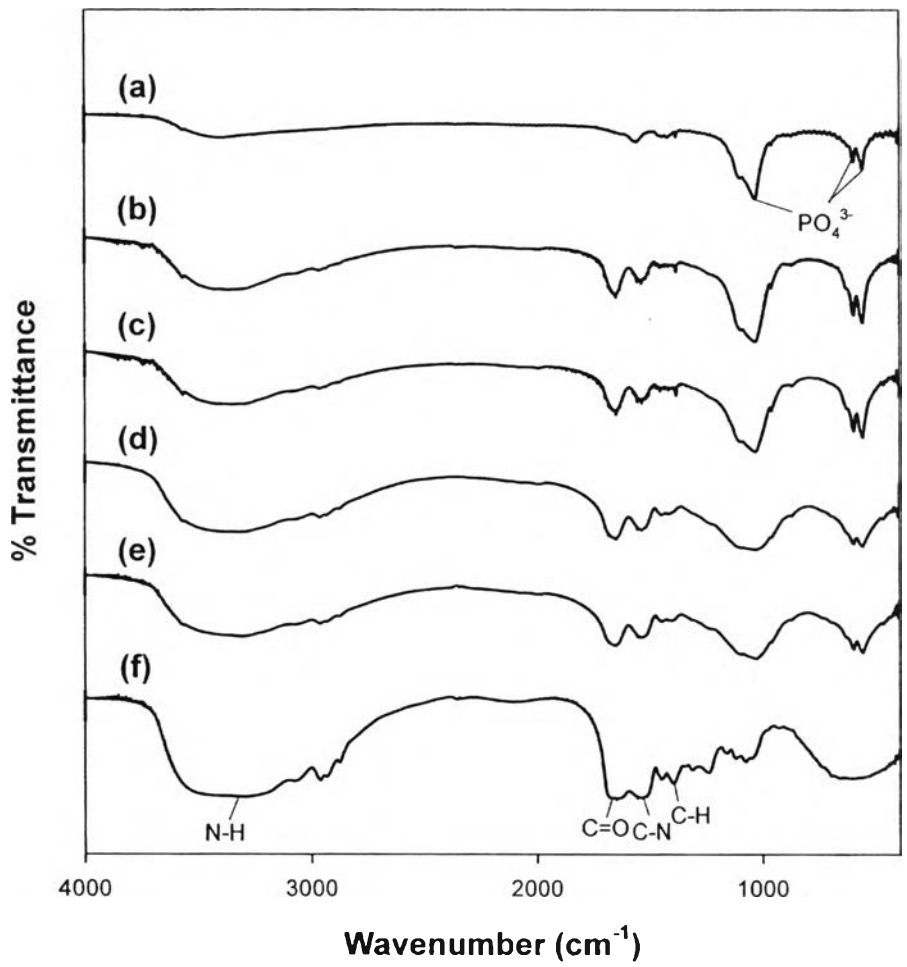


**Figure 5.2** FT-IR spectra of (a) 0D-7, (b) 1D-7, (c) 1D-9, (d) 1E-7, (e) 1E-9, and (f) as-received OVA in its dry state.

EDX analysis was performed to give further confirmation of a molar Ca/P ratio of the samples. The EDX characteristic peaks indicated the existence of calcium (Ca) and phosphorous (P) with proportional counts (see Figure 5.3). The average molar Ca/P ratio of the obtained samples synthesized by using the chemical starting material are in the range of 1.67-1.68, which is very close to the ideal one of

1.67 for HAp in human bone, while those of the obtained samples synthesized from the natural starting material are in the range of 1.62-1.65. Nonetheless, there were not statistically significant differences of the average molar Ca/P ratio of both starting materials.

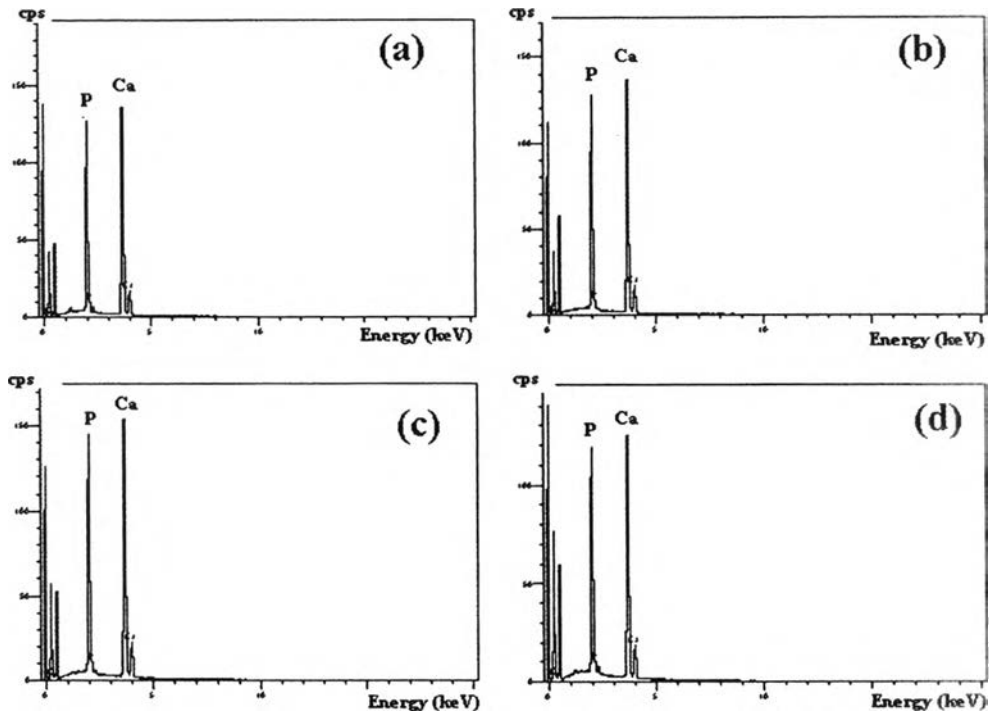


**Figure 5.3** EDX characteristic peaks of (a) 1D-7, (b) 1D-9, (c) 1E-7, and (d) 1E-9.

The HAp/OVA particles were also examined by transmission electron microscopy (TEM). The representative TEM micrographs of the samples synthesized from both starting materials at pH 7 and 9 with the initial OVA amount of 1 g show little difference in morphology (see Figure 5.4). For all the obtained samples, the primary particles have a rod-like shape with dimensions of 3–10 nm in diameter and 15–30 nm in length. However, it was noticed that the sizes of primary particles slightly increase with a higher amount of OVA initially added and a lower pH condition.

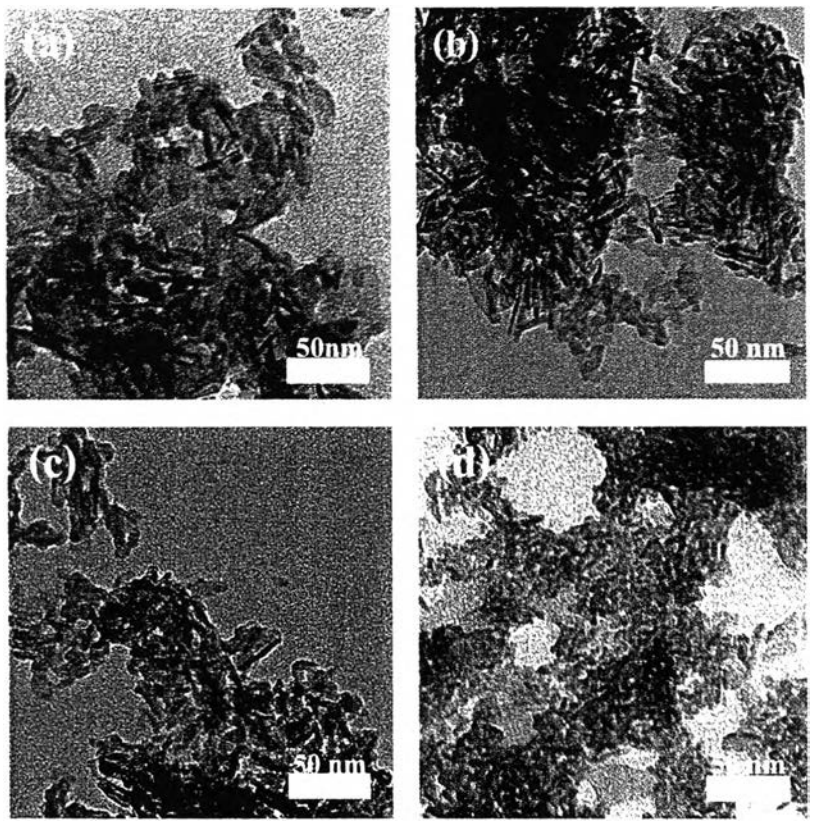


**Figure 5.4** Representative TEM micrographs of (a) 1D-7, (b) 1D-9, (c) 1E-7, and (d) 1E-9.

5.4.2 OVA-Incorporating Determination

The physi-sorption of nitrogen was performed to collect the average pore diameters of the pure HAp and HAp/OVA particles (see Table 5.2). The average pore sizes of HAp particles with the presence of OVA are larger than those of the absence ones, suggesting the incorporation of OVA within HAp particles by bond formation. The mechanism was that the carbonyl group and the phosphorous group of OVA have negative dipoles which could chelate the free $Ca^{2+}$ ions; subsequently, the $PO_4^{3-}$ ions may bond with OVA-associated calcium to generate HAp/OVA aggregates (Zhao *et al.*, 2008). OVA, furthermore, could be adsorbed on the HAp surfaces by the crystal surface area available for growth (Ijntema *et al.*, 1994). When considering HAp/OVA particles, the average pore diameters at lower pH are bigger than those at higher pH. At the same pH, the average pore diameters of

the HAp/OVA particles synthesized from the chemical starting material display the higher values than those of the HAp/OVA particles synthesized from the natural one. The average pore diameters, nevertheless, are quite similar in case of varying the initial amounts of OVA. Therefore, it could be assumed that the difference in these initial amounts of OVA added has a little influence on the average pore size.

For thermal behavior, TGA profiles of the obtained HAp and HAp/OVA powders prepared in several conditions are presented in Figure 5.5. The mass loss could be differentiated into four regions in the investigated temperature range of (1) 60–200°C, (2) 200–400 °C, (3) 400–780 °C, and (4) 780–1200 °C. The mass loss below 200 °C was attributed to the loss of adsorbed water. From 200–400 °C, an obvious mass loss was detected due to the loss of tris- base (endothermic peak around 240 °C), OVA (endothermic peak around 330 °C), and other absorbed species. The mass loss between 400 and 780 °C corresponded to the decomposition of remained organic residues was rather small for all particulate HAp samples. Above 780 °C, a very small transition was mainly attributed to the weight loss of carbonate. The actual contents of OVA incorporated within HAp particles based on the total amount of 5 mg of the dried samples are shown in Table 5.2. All these values could be determined from the TGA result, which were in the range of 5.24–8.01, 6.01–9.32, and 6.39–9.94% for the initial amounts of OVA added of 1, 2, and 3 g, respectively, for the HAp/OVA particles synthesized from both starting materials at both pH. The theoretical contents of OVA incorporated into HAp particles synthesized from both starting materials are around 26, 42, and 52 wt% for 1, 2, and 3 g of the initial amounts of OVA added, respectively. For all the obtained samples, the mass loss slightly increased when increasing the initial amounts of OVA, which meant that the amounts of OVA incorporated did not significantly increase with the increase of the initial contents of OVA. However, a larger quantity of OVA incorporated was noticed in the HAp/OVA particles synthesized from the chemical starting material compared to those prepared from the natural one. The type of starting material, therefore, caused honestly significant differences in the OVA-incorporated content ($p < 0.05$). A lower pH in the synthesis procedure resulted in a significantly greater amount of OVA incorporated for both starting materials ($p < 0.05$) because there is the electrostatic repulsion force between OVA and HAp,

which predominates in a higher pH solution (pH 9) compared to a lower pH solution (pH 7). As a result, the increase in pH solution decreased the amount of OVA incorporated (Liu *et al.*, 2005).

**Table 5.2** Physico-chemical characteristics of HAp and HAp/OVA particles

| Sample | Average Pore Diameter (nm) | OVA-Incorporated Amount (%) | OVA-Released Amount (%) |
|---|---|---|---|
| 0D-7 | 9.43 ± 0.02 | - | - |
| 1D-7 | 16.4 ± 0.15 | 8.01 ± 0.92 | 57.5 ± 3.71 |
| 2D-7 | 16.8 ± 0.11 | 9.32 ± 0.37 | 60.0 ± 4.10 |
| 3D-7 | 16.9 ± 0.07 | 9.94 ± 0.96 | 62.0 ± 3.82 |
| 0D-9 | 8.69 ± 0.14 | - | - |
| 1D-9 | 13.7 ± 0.18 | 7.54 ± 0.83 | 42.1 ± 2.73 |
| 2D-9 | 14.2 ± 0.06 | 7.99 ± 0.68 | 43.7 ± 2.90 |
| 3D-9 | 14.8 ± 0.03 | 8.21 ± 0.74 | 44.0 ± 1.95 |
| 0E-7 | 8.91 ± 0.19 | - | - |
| 1E-7 | 15.0 ± 0.14 | 6.17 ± 0.45 | 50.1 ± 3.06 |
| 2E-7 | 15.3 ± 0.27 | 7.61 ± 0.33 | 52.6 ± 2.81 |
| 3E-7 | 15.6 ± 0.29 | 8.89 ± 0.87 | 54.2 ± 3.66 |
| 0E-9 | 8.18 ± 0.03 | - | - |
| 1E-9 | 13.5 ± 0.22 | 5.24 ± 0.72 | 38.8 ± 1.13 |
| 2E-9 | 13.9 ± 0.26 | 6.01 ± 0.79 | 40.3 ± 2.09 |
| 3E-9 | 14.3 ± 0.15 | 6.93 ± 0.44 | 40.8 ± 1.84 |

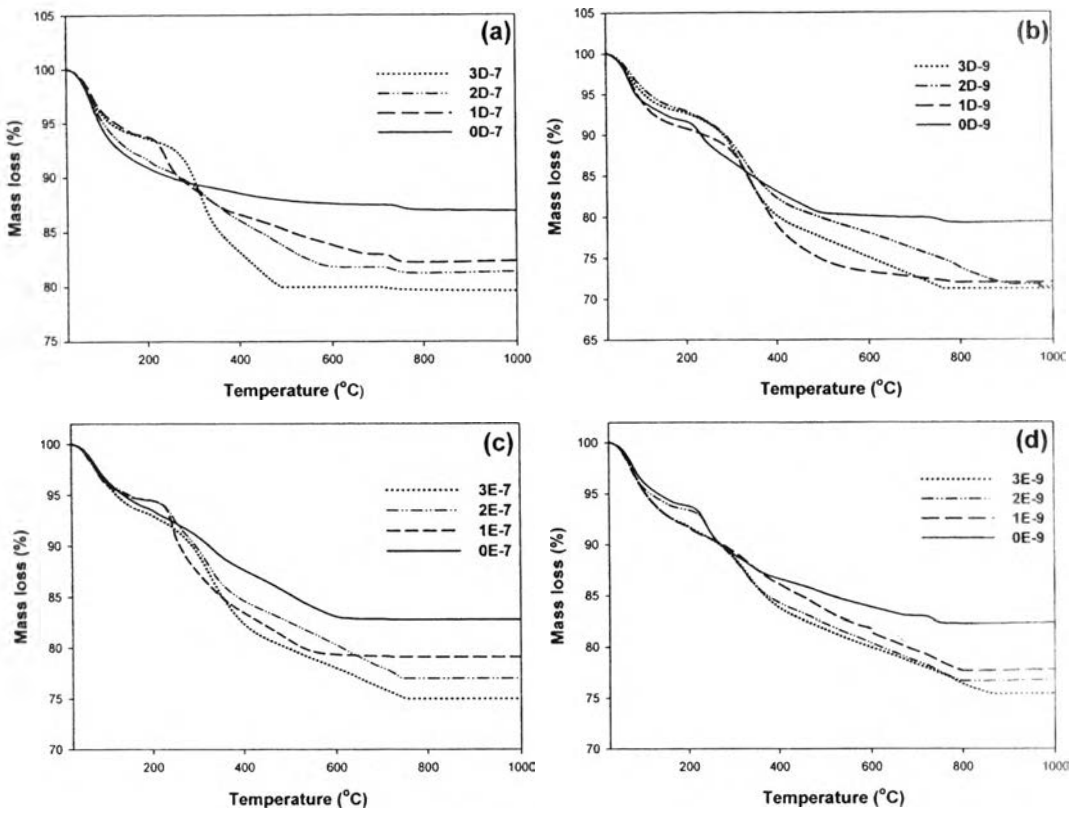


**Figure 5.5** TGA profiles of HAp and HAp/OVA particles synthesized at various conditions.

5.4.3 Release Kinetics of Ovalbumin

The release experiments of OVA, carried out in PBS (pH 7.4) to simulate the local pH of the homeostatic body fluid, were performed for all particulate HAp and HAp/OVA. The release profiles and the release amounts of OVA based on the amounts of OVA incorporated into HAp particles are shown in Figure 5.6 and Table 5.2, respectively. It was found that the obtained HAp/OVA particles prepared from both starting materials demonstrated a slow release behavior increased time dependently within 21 days; a plateau release was then followed and the burst release was not observed. The single-stage release profiles of OVA were assigned to the OVA molecules incorporated into HAp particles (HAp/OVA complex) (Liu *et al.*, 2005). The complex was formed by the adsorption of OVA on the Ca-site of HAp by ionic interaction between carboxyl acid groups on OVA and

the positively charged Ca-sites. Phosphate ions from PBS can be also adsorbed onto the Ca-sites, so the competition between acidic protein molecules and phosphate ions occurs, resulting in OVA desorption from the HAp/OVA particles (Kawasaki, 1990; Akasawa, 1996). The sustained release profiles of OVA, moreover, can be possibly attributed to the formation of porous structure of HAp particles. The release values of OVA from the HAp/OVA particles synthesized from the natural starting material after 35 days at pH 7 and 9 were about 50–54% and 38–41%, respectively. A more sustained OVA release was fulfilled for the HAp/OVA particles prepared from the chemical starting material. Around 57–62% and 42–44% of OVA were released out after the same period of time for pH 7 and 9, respectively. The amounts of OVA released from the chemical starting material were significantly greater than those released from the natural one ($p < 0.05$). The statistically higher amounts of OVA released were also observed at pH 7 than those observed at pH 9 ($p < 0.05$). This is because a smaller amount of tris-base added led to a looser and weaker bond formation. Therefore, the quantity of OVA released considerably relies on the pH condition and the type of the starting material. All of the release patterns also revealed the incomplete release of OVA owing to its instability problems such as non-specific adsorption and aggregation (Kim *et al.*, 2004). Even though a higher amount of OVA initially added provided a slightly higher amount of OVA released depending on the actual content of OVA incorporated, the release values of OVA were statistically the same.

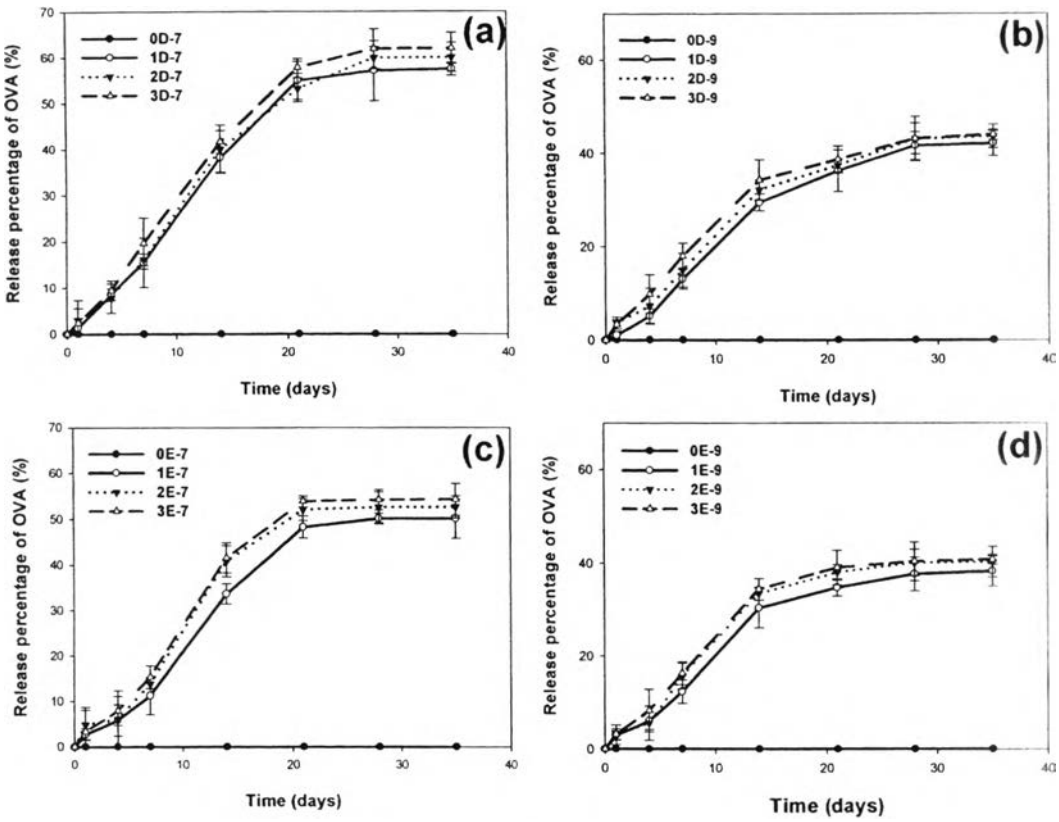


**Figure 5.6** Release profiles of OVA from the obtained HAp/OVA particles synthesized under different conditions.

## 5.5 Conclusions

Protein carriers based on HAp particles were designed as potential devices for the controlled release system. HAp/OVA particles were successfully synthesized by the co-precipitation method with different starting materials, pH values, and initial amounts of OVA added. The amounts of OVA both incorporated and released statistically increased with the decrease of pH value to be neutral and slightly increased with the increase in the initial amount of OVA added. A greater amount of OVA both incorporated and released was also observed in the HAp/OVA particles synthesized from the chemical starting material compared to those prepared from the natural one. The release kinetics exhibited a slow release in a sustained manner

without initial OVA burst, resulting in prolonged release behavior. Consequently, it may be practicable to use the obtained HAp particles with other protein drugs and growth factors as effective carries to achieve specific targets for bone tissue engineering purposes.

## 5.6 Acknowledgments

The authors acknowledge the partial support received from 1) The Thailand Research Fund (TRF, grant no.: DBG5280015), 2) The Institute for the Promotion of Teaching Science and Technology (IPST, for the doctoral scholarship of P.K.), 3) The Petroleum and Petrochemical College (PPC), Chulalongkorn University, and 4) Center of Excellence on Petrochemical and Materials Technology (PETRO-MAT), Chulalongkorn University.

## 5.7 References

Akasawa, T. and Kobayashi, M. (1996) Surface characteristics of hydroxyapatite controlling albumin adsorption behavior. Journal of Materials Science Letters, 15, 1319-1320.

Bose, S. and Saha, S.K. (2003) Synthesis of hydroxyapatite nanopowders via sucrose-templated sol- gel method. Journal of the American Ceramic Society, 86, 1055-1057.

Carutenuto, G., Spagnuolo, G., Ambrosio, L., and Nicolais, L. (1999) Mesoporous hydroxyapatite as alloplastic material for dental applications. Journal of Materials Science: Materials in Medicine, 10, 671-676.

Djosic, M.S., Miskovic-Stankovic, V.B., Milonjic, S., Kacarevic-Popovic, Z.M., Bibic, N., and Stojanovic, J. (2008) Electrochemical synthesis and characterization of hydroxyapatite powders. Materials Chemistry and Physics, 111, 137-142.

He, W., Li, Z.M., Wang, Y.J., Chen, X.F., Zhang, X.D., Zhao, H.S., Yan, S.P., and Zhou, W.J. (2010) Synthesis of mesoporous structured hydroxyapatite

particles using yeast cells as the template. Journal of Materials Science: Materials in Medicine, 21, 155-159.

IJntema, K., Heuvelsland, W.J.M., Dirix, C.A.M.C., and Sam, A.P. (1994) Hydroxyapatite microcarriers for biocontrolled release of protein drugs. International Journal of Pharmaceutics, 112, 215-224.

Jalota, S., Bhaduri, S.B., and Tas, A.C. (2007) A new rhenanite (β-$NaCaPO_4$) and hydroxyapatite biphasic biomaterial for skeletal repair. Journal of Biomedical Materials Research Part B: Applied Biomaterials, 80, 304-316.

Kawasaki, T., Niikura, M., and Kobayashi, Y. (1990) Fundamental study of hydroxyapatite high- performance liquid chromatography: II. Experimental analysis on the basis of the general theory of gradient chromatography. Journal of Chromatography, 515, 91-123.

Kim, H.K. and Park, T.G. (2004) Comparative study on sustained release of human growth hormone from semi-crystalline poly(L-lactic acid) and amorphous poly(D,L-lactic-co-glycolic acid) microsphere: morphological effect on protein release. Journal of Controlled Release, 98, 115-125.

Kokubo, T., Kim, H.M., and Kawashita, M. (2003) Novel bioactive materials with different mechanical properties. Biomaterials, 24, 2161-2175.

Koumoulidis, G.C., Katsoulidis, A.P., Ladavos, A.K., Pomonis, P.J., Trapalis, C.C., Sdoukos, A.T., and Vaimakis, T.C. (2003) Preparation of hydroxyapatite via microemulsion route. Journal of Colloid and Interface Science, 259, 254-260.

Krisanapiboon, A., Buranapanitkit, B., and Oungbho, K. (2006) Biocompatibility of hydroxyapatite composite as a local drug delivery system. Journal of Orthopaedic Surgery, 14, 315-318.

Liu, T.Y., Chen, S.Y., Liu, D.M., and Liou, S.C. (2005) On the study of BSA-loaded calcium- deficient hydroxyapatite nano-carriers for controlled drug delivery. Journal of Controlled Release, 107,112-121.

Liu, Y., Layrolle, P., De Bruijn, J., Blitterswijk, C.V., and De Groot, K. (2001) Biomimetic coprecipitation of calcium phosphate and bovine serum albumin on titanium alloy. Journal of Biomedical Materials Research, 57, 327-335.

Rivera, E.M., Araiza, M., Brostow, W., Castano, V.M., Diaz Estra, J.R., Hernandez, R., and Rodriguez, J.R. (1999) Synthesis of hydroxyapatite from egg shells. Materials Letters, 41, 128-134.

Santos, C., Franke, R.P., Almeida, M.M., Costa, M.E.V. (2003) Nanoscale characterization of hydroxyapatite particles by electron microscopy. Microscopy and Microanalysis, 14, 67-70.

Shum, H.C., Bandyopadhyay, A., Bose, S.,and Weitz, D.A. (2009) Double emulsion droplets as microreactors for synthesis of mesoporous hydroxyapatite. Chemistry of Materials, 21, 5548-5555.

Sivakumar, M. and Rao, K.P. (2002) Preparation, characterization and in vitro release of gentamicin from coralline hydroxyapatite-gelatin composite microsphere. Biomaterials, 23, 3175-3181.

Sopyan, I., Mel, M., Ramesh, S., and Khalid, K.A. (2007) Porous hydroxyapatite for artificial bone applications. Science and Technology of Advanced Materials, 8, 116-123.

Suru, V.M., Ng, C.H., Wilke, M., Tiersch, B., Fratzl, P., and Peter, M.G. (2005) Size-controlled hydroxyapatite nanoparticles as self-organized organic-inorganic composite materials. Biomaterials, 26, 5414-5426.

Suwa, Y., Banno, H., Mizuno, M., and Saito, H. (1993) Synthesis of compositionally regulated hydroxyapatite from $Ca(OH)_2$ and $H_3PO_4$. Journal of Ceramic Society of Japan, International Edition, 101, 642-647.

Viswanath, B. and Ravishankar, N. (2008) Controlled synthesis of plated-shape hydroxyapatite and implications for the morphology of the apatite phase in bone. Biomaterials, 29, 4855-4863.

Wang, H.N., Li, Y.B., Zuo, Y., Li, J.H, Ma, S.S., and Cheng, L. (2007) Biocompatibility and osteogenesis of biomimetic nano-hydroxyapatite/polyamide composite scaffolds for bone tissue engineering. Biomaterials, 28, 3338-3348.

Wang, Y.J., Chen, J.D., Wei, K., Zhang, S.H., and Wang, X.D. (2006) Surfactant-assisted synthesis of hydroxyapatite particles. Materials Letters, 60, 3227-3231.

Xu, Q.G., Tanaka, Y., and Czernuszka, J.T. (2007) Encapsulation and release of a hydrophobic drug from hydroxyapatite coated liposome. Biomaterials, 28, 2687-2694.

Ye, F., Guo, H.F., and Zhang, H.J. (2008) Biomimetic synthesis of oriented hydroxyapatite mediated by nonionic surfactants. Nanotechnology, 19, 245605.

Zhao, H.S., He, W., Wang, Y.J., Zhang, X.D., Li, Z.M., Yan, S.P., and Zhao, W.J (2008) Biomimetic synthesis and characterization of hydroxyapatite crystal with low phase transformation temperature. Journal of Chemical and Engineering Data, 53, 2735-2738.

Zhao, H.S., He, W., Wang, Y.J., Zhang, X.D., Li, Z.M., Yan, S.P., Zhou, W.J., and Wang, G.C. (2008) Biomineralization of large hydroxyapatite particles using ovalbumin as biosurfactant. Materials Letters, 62, 3603-3605.